Bio-Inspired Balance Control Assistance Can Reduce Metabolic Energy Consumption in Human Walking

Guoping Zhao, Maziar Ahmad Sharbafi, Mark Vlutters, Edwin van Asseldonk, and Andre Seyfarth

***Abstract*— The amount of research on developing exoskeletons for human gait assistance has been growing in the recent years. However, the control design of exoskeletons for assisting human walking remains unclear. This paper presents a novel bio-inspired reflex-based control for assisting human walking. In this approach, the leg force is used as a feedback signal to adjust hip compliance. The effects of modulating hip compliance on walking gait is investigated through joint kinematics, leg muscle activations and overall metabolic costs for eight healthy young subjects. Reduction in the average metabolic cost and muscle activation are achieved with fixed hip compliance. Compared to the fixed hip compliance, improved assistance as reflected in more consistent reduction in muscle activities and more natural kinematic behaviour are obtained using the leg force feedback. Furthermore, smoother motor torques and less peak power are two additional advantages obtained by compliance modulation. The results show that the proposed control method which is inspired by human posture control can not only facilitate the human gait, but also reduce the exoskeleton power consumption. This demonstrates that the proposed bio-inspired controller allows a synergistic interaction between human and robot.**

***Index Terms*— Virtual pivot point, force modulated compliant hip, exoskeleton, bio-inspired control, human gait, assistive device.**

I. Introduction

HUMAN locomotor systems comprise complex but intensively coupled mechanics and control to achieve gaits such as walking and running. As walking is the most common gait in daily life, assisting walking could be a way to overcome mobility related physical and functional losses [1]. In order to assist human gait with an exoskeleton, the exoskeleton should be controlled in a way that humans can easily utilize the provided torque/force for the motion. As the exoskeleton is attached to human body, human states have to be taken into account for the control of the robot. Basic control principles of human locomotion can provide guidelines for designing assistive controllers.

Human locomotion control can be divided into reflexes (feedback, e.g. force, displacement and velocity reflexes) and central pattern generators (CPGs, i.e. feedforward) generated by the central nervous system and the preflex responses resulting from muscle dynamics [2]–[4]. It has been shown that the locomotion behaviors in humans and other legged animals are highly depended on the neural circuits in the spinal cord [5], [6]. The CPGs can be considered as the neural circuits in the spinal cord which can generate rhythmic muscle activation patterns without any feedback inputs [3], [7]. However, it is not required to have CPGs to produce a sequence of muscle activation patterns for locomotion. With neuromuscular simulation models, Geyer et al. showed that a pure reflex-based control (sensory feedback integration) can produce stable and diverse behaviors of human locomotion including walking and running gait [8], [9]. The balance control of the model was realized by manually defined complex muscle reflex pathways. In contrast, a simplified conceptual model with spring-like prismatic legs and compliant hips can also generate human-like walking gait and balance the trunk by a simple leg force based reflex control of the hip compliance [10].

Here we focus on human-inspired posture control approaches for exoskeletons and their benefits for walking. Posture control is one of the human locomtor sub-functions [11]. We believe that with posture control assistance not only stability but also energetics can be improved as locomotor sub-functions are internally connected with each other. As falling injuries are more critical than energetic drawbacks for elderly, targeting improving posture is the more important functionality compared to targeting the walking energetics.

Several control approaches that have been implemented on exoskeletons to assist human walking [12]: 1) Predefined trajectory tracking based approaches. For instance, ATLAS orthoses [13], HAL [14], Mina [15], Mindwalker [16], ReWalk [17], and eLEGS [18] for assisting pathological gaits. 2) Predefined gait pattern based control. As in the soft exosuit control in [19], [20], the desired assistance depends not

Manuscript received April 12, 2019; revised June 14, 2019; accepted July 15, 2019. Date of publication August 12, 2019; date of current version September 6, 2019. This work was supported in part by the Seventh Framework Program (FP7) of the European Commission (Information and Communication Technologies, ICT-2011.2.1) through the Balance Augmentation in Locomotion, through Anticipative, Natural and Cooperative control of Exoskeletons (BALANCE) Project under Grant 601003, in part by the EU-Funded BALANCE Project under Grant FP7-ICT-2011.2.1 and Grant 601003, and in part by the DFG-Funded EPA Project under Grant AH307/2-1 and Grant SE1042/29-1. *(Corresponding author: Guoping Zhao.)*

G. Zhao and A. Seyfarth are with the Lauflabor Locomotion Laboratory, Centre for Cognitive Science, Institute of Sport Science, Technische Universität Darmstadt, 64289 Darmstadt, Germany (e-mail: zhao@sport.tu-darmstadt.de).

M. Ahmad Sharbafi is with the Lauflabor Locomotion Laboratory, Centre for Cognitive Science, Institute of Sport Science, Technische Universität Darmstadt, 64289 Darmstadt, Germany, and also with the Control and Intelligent Processing Center of Excellence (CIPCE), School of Electrical and Computer Engineering, University of Tehran, Tehran 14395/515, Iran.

M. Vlutters and E. van Asseldonk are with the Department of Biomechanical Engineering, University of Twente, 7500 Enschede, The Netherlands.

This article has supplementary downloadable material available at http://ieeexplore.ieee.org, provided by the authors.

Digital Object Identifier 10.1109/TNSRE.2019.2929544

This work is licensed under a Creative Commons Attribution 4.0 License. For more information, see http://creativecommons.org/licenses/by/4.0/

only on the timing of the control command but also on the characteristics of the elastic elements (stiffness, inertia, damping). 3) Model based approaches in which the desired robotic action is computed on the basis of a human-exoskeleton model. These approaches usually consider gravity compensation, zero moment point (ZMP) balance criterion, and provide extra commanded assistance which requires highly precise models and multiple sensors to recognize human body kinematics and dynamics variables [12], e.g. in [21]–[24]. 4) Adaptive oscillators-based control (basic concept used in CPG) [25], which is limited to subjects who can deliver periodic and stable locomotion-related signals, and mostly validated on the hip joint actuation [26]–[30]. 5) Proportional myoelectrical control for single joint exoskeletons, e.g. Fleischer and Hommel [31], Norris *et al.* [32], and Kao *et al.* [33]. 6) Hybrid strategies, including aforementioned methods. E.g. BLEEX adopts a force controller in swing phase and a position controller in stance phase [34]; or combination of fuzzy control with other methods [35]–[39]. None of these methods take the basic control principles of human locomotion as the basis for the control of exoskeletons. Recent studies have shown that exoskeletons with neuromuscular controller which use lower limb dynamic model [40]–[42] can assist human walking. But this method requires complex neuromuscular modelling of major leg muscle groups.

In this paper, we introduce a simple bio-inspired reflex based control design in gait assistance which is developed based on a human balance control. One phenomenon observed in biological gaits that can be considered as a basis for our bio-inspired balance control is the virtual pendulum (VP) concept [43]. Maus et al. showed that during human walking the ground reaction force vectors are pointing to a virtual pivot point (VPP) which is placed above the center of mas (CoM). With that the upper body oscillates stably and mimics the periodic motion of a regular pendulum. The VPP control concept can be approximated by the force modulated compliant hip (FMCH) control [10], [44] during walking and running. The FMCH controller uses the leg force to adjust the hip stiffness which mimics force reflexes in human body. This simple reflex-based controller can generate human-like hip flexion/extension torque patterns for walking.

In the previous pilot study we have tested the FMCH based controller with both hip and knee assistance for walking [45]. We also implemented this concept using a biarticular thigh actuator with a neuromuscular model [46]. Both results showed that this approach is feasible to implement and can reduce both human metabolic costs and leg muscle activation. However, the individual contributions of hip and knee joint to the reductions are unclear. It also remains open whether a single joint (i.e. hip or knee joints) FMCH based assistance controller can reduce metabolic costs. It has been shown that human hip joint contributes more than 40% of positive work during walking (from 0.75 m/s to 2.00 m/s) [47]. Therefore, in this paper, we focus on assisting only the hip joint.

The aim of this paper is to investigate the implementation and the resulting benefits of a human bio-inspired posture control scheme for assisting human walking. In this study, we are focusing on assisting only the hip joints to investigate the benefits of FMCH based controller for walking energetics. In addition, we also investigate the importance of leg force feedback for the assistive controller. This is achieved by comparing the results of the FMCH and the constant compliant hip (CCH) control (without force feedback).

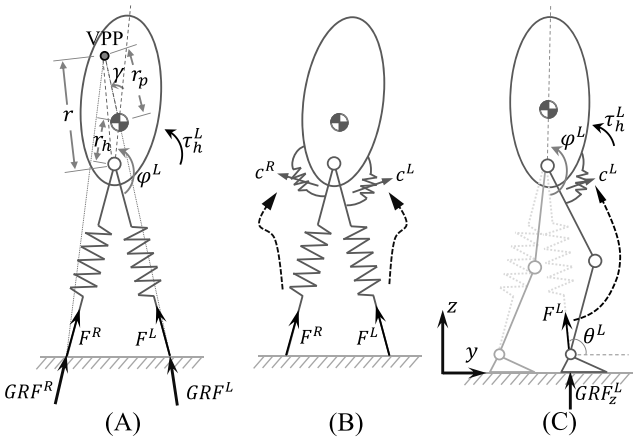

Fig. 1. Bio-inspired walking models. (A) Virtual pivot point (VPP) model [43]. (B) Force modulated compliant hip (FMCH) model [10]. (C) The FMCH based hip torque control implemented in this study.

More specifically, we employ the FMCH concept to control the hip actuator of the exoskeleton LOPES II. This method is compared with CCH. The results demonstrate the effects of these two control methods on metabolic costs, muscle activation and kinematic behavior. Finally, the effects of the leg force feedback (used as a reflex pathway) on the aforementioned human locomotion metrics, together with the impacts on efficiency of the methods, will be assessed by the consumed power and produced torques of the exoskeleton and discussed.

II. Methods

A. Control Concepts

The VPP walking model consists of a rigid trunk and two massless spring-like prismatic legs (Fig. 1A). Each hip joint torque can be computed as [43]:

$$\tau_h = Fl\frac{r_h \sin\varphi + r_p \sin(\varphi+\gamma)}{l - r_h\cos\varphi - r_p\cos(\varphi+\gamma)} \tag{1}$$

where τ_h is hip torque, F is leg force, l is leg length, φ is hip angle, r_p is the distance from CoM to VPP, and r_h is the distance from CoM to hip joint. γ denotes the angle between trunk axis and the vector from CoM to VPP. Left or right hip torque (τ_h^L or τ_h^R) can be computed by substituting (F, l, φ) in (1) with $\left(F^L, l^L, \varphi^L\right)$ or $\left(F^R, l^R, \varphi^R\right)$, where the superscript L and R denote the left and right leg, respectively.

The VPP model can be approximated by the FMCH model (Fig. 1B) if $\gamma < 20°$ and $150° < \varphi^{L,R} < 210°$ [10]. This approximation can be made during regular walking [10]. A variable stiffness rotational spring was used in the FMCH

Fig. 2. A subject walking with LOPES II exoskeleton.

model to produce a similar hip torque pattern which results in a similar VPP position above the CoM. The hip torque can be computed with the following equation by assuming the hip spring stiffness is multiplied by the leg force F [10]:

$$\tau_h = cF(\varphi_0 - \varphi) \tag{2}$$

where c and φ_0 denote nominal hip spring stiffness (constant, normalized to body weight) and rest angle, respectively.

B. Implementation

The FMCH based hip torque control (2) was implemented on the exoskeleton LOPES II. This control is simpler while it has similar performance compared to (1) [10]. LOPES II consists of a pair of shadow legs which can apply active hip flexion/extension torques on the human body with the low-level admittance controller (Fig. 2, see [48] for details). The instrumented treadmill provides the net vertical ground reaction force GRF_z^T and the net center of pressure position $\left(x_{cop}^T, y_{cop}^T\right)$ feedback to the control system (see Fig. 3). The left-right, fore-aft and vertical direction are denoted as x-axis, y-axis and z-axis (Fig. 1C), respectively.

Each leg force magnitude F is estimated as:

$$F = GRF_z \big/ \sin\theta \tag{3}$$

where GRF_z and θ denote the individual leg vertical GRF and the leg angle with respect to the horizontal direction, respectively. θ is estimated as:

$$\theta = \arccos \frac{y_h - y_a}{|\mathbf{p}_h - \mathbf{p}_a|} \tag{4}$$

where $\mathbf{p}_h$ and $\mathbf{p}_a$ denote the position of hip (x_h, y_h, z_h) and ankle (x_a, y_a, z_a) joint in the global Cartesian space. They can be measured by LOPES II.

Individual leg GRF_z equals to GRF_z^T during the single stance phase. In the double stance phase, the individual leg

TABLE I
PARAMETER VALUES USED IN THE EXPERIMENT

Parameter	Value [unit]
$\hat{c}$	$0.035\,\mathrm{rad}^{-1}$
φ_0	$3.264\,\mathrm{rad}$

GRF_z is estimated by assuming the projection of each ankle joint on the ground as the individual leg CoP position:

$$\begin{bmatrix} GRF_z^L \\ GRF_z^R \end{bmatrix} = \begin{bmatrix} |y_{cop}^T - y_a^R| \\ |y_{cop}^T - y_a^L| \end{bmatrix} \frac{GRF_z^T}{\left|y_a^L - y_a^R\right|} \tag{5}$$

The desired hip flexion/extension torque applied by the exoskeleton τ_{hExo} can be computed by combining (2-5). To accommodate for differences in subject height h, we normalized the hip stiffness c with h:

$$\tau_{hExo} = h\hat{c}F\,(\varphi_0 - \varphi) \tag{6}$$

φ in (2) is the virtual hip angle which is the angle between trunk axis and the vector from ankle to the hip joint (shown in Fig. 1C). In LOPES II, the trunk axis angle is fixed and set to zero. Ankle position $\mathbf{p}_a$ was used to detect stance and swing phase of each individual leg [49], [50].

The controller has two parameters $\left(\hat{c}, \varphi_0\right)$ for each leg. In this study we set each parameter to the same value for both legs by assuming subjects walk symmetrically. In order to find appropriate control parameters, we hand-tuned the parameters based on the previous study [45] for two pilot subjects before the experiment by gradually increasing the parameters till both of them felt most comfortable. The parameter values used in the experiment are shown in Table I. The test subjects did not participate in the experiment.

In order to investigate the effectiveness of the force modulation in FMCH controller on human walking gait, we also implemented a constant compliant hip (CCH) controller in which the leg force was set to a constant value (subject body weight):

$$\tau_{hExo} = h\hat{c}mg\,(\varphi_0 - \varphi) \tag{7}$$

where m and g denotes subject body mass and gravitational acceleration.

Both FMCH and CCH controllers were implemented in Matlab (R2015b, MathWorks) using Simulink Real-time toolbox with a control frequency of 1 kHz.

C. Experimental Protocol

Eight subjects (5 females, 3 males, age 26 ± 4.0 years, height $1.75 \pm 0.04\,\mathrm{m}$, weight $67.9 \pm 6.2\,\mathrm{kg}$, mean ± std.) participated in this study. All subjects were healthy without any known neuromuscular injury or functional impairment. They had no previous experience of walking with FMCH or CCH controller in LOPES II. They voluntarily signed an informed consent form approved by the Medical Ethics Committee Twente.

In order to familiarize with the exoskeleton and the experimental setup, each subject had a test walking trail (5 min) with

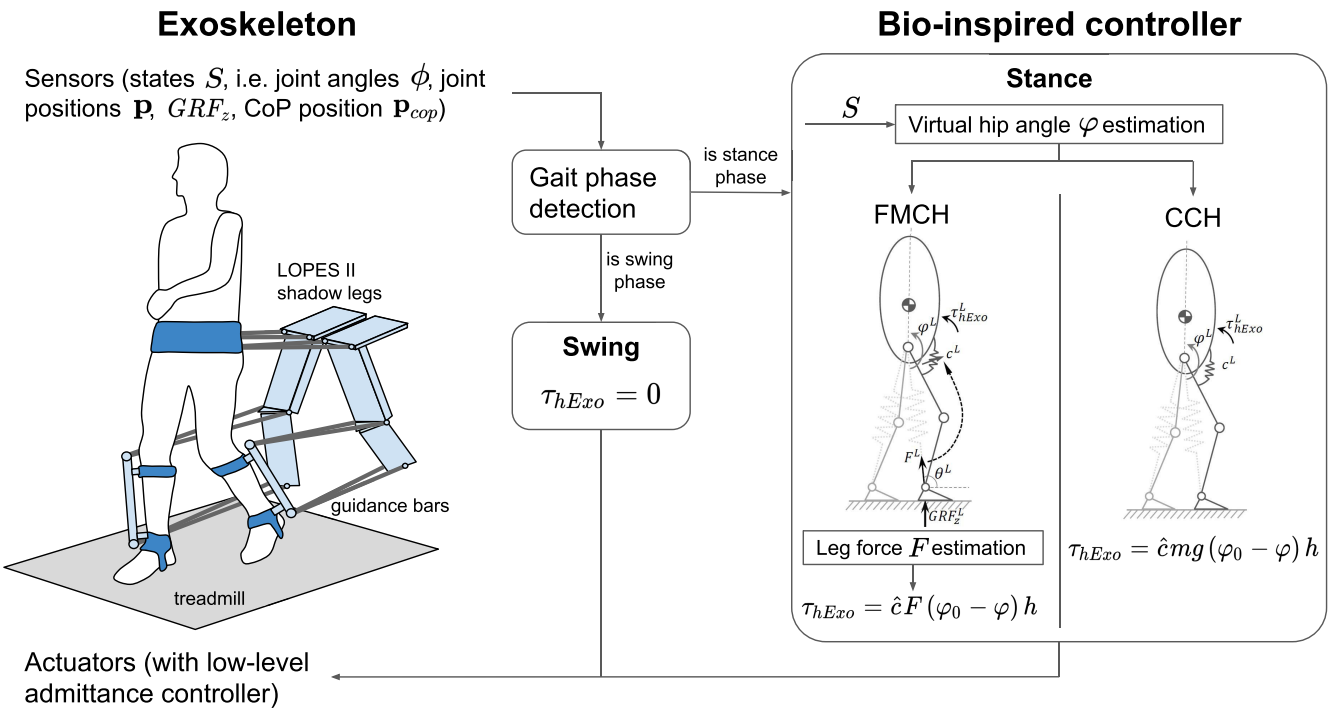

Fig. 3. Schematic overview of FMCH and CCH controller. Sensors on the exoskeleton are used to detect if the leg is in stance or swing phase. The exoskeleton is set to transparent mode (hip joint torque is set to zero) if the leg is in swing phase. FMCH or CCH controller is activated if the leg is in stance phase.

the exoskeleton in transparent, FMCH and CCH mode. Then subjects had 5 min resting time before the experimental trials. During the experiment, subjects were instructed to wear the exoskeleton and walk on the treadmill with natural arm swing at a constant speed of 0.7 m/s. The speed is limited due to safety constraints of LOPES II. At the beginning of walking trials, a 3 min standing (wearing the exoskeleton) session was performed to measure the baseline (steady-state standing) metabolic cost. Then subjects walked for three 7-minute bouts, i.e. walking with transparent, FMCH, and CCH controller. Subjects rested for about 3 min in between walking bouts to prevent fatigue. The three walking bouts were randomized to avoid baseline and learning effects.

Subject hip and knee kinematic data and human-exoskeleton interaction torques were collected by LOPES II at 1 kHz. Seven right leg muscles (tibialis anterior (TIA), soleus (SOL), medial gastrocnemius (GAS), vastus medialis (VAS), rectus femoris (REC), hamstring (HAM), and gluteus maximus (GLU)) surface electromyography (EMG) signals were recorded (Delsys Inc., Natick, USA) at 1 kHz. Metabolic cost rate was assessed by measuring subject oxygen consumption rate and carbon dioxide output rate evey ten seconds (K5, Cosmed, Roma, Italy).

D. Data Processing

To avoid adaptation effects, only the last three minutes of data in each condition were processed and analyzed. EMG data were high-pass filtered at 20 Hz (4th order zero-lag Butterworth), detrended, rectified, and then low-pass filtered at 6 Hz (4th order zero-lag Butterworth). Then each muscle EMG data were normalized to the average maximum EMG value during all the gait cycles in the transparent mode. The root mean square (r.m.s) of muscle EMG during each gait cycle was computed to quantify changes in EMG amplitude and indicate muscle activation level. Then each muscle r.m.s EMG data were normalized to the mean r.m.s EMG in the transparent condition. Joint angles and exoskeleton hip torques were low-pass filtered at 20 Hz and 4 Hz (4th order zero-lag Butterworth), respectively. The exoskeleton hip mechanical power was computed by multiplying exoskeleton hip torque and the time derivative of hip angle. The mean and standard deviation of exerted joint torque and power were computed after normalizing the data to each subject's body mass. The metabolic cost rate was calculated using the Brockway equation [51]. For better presenting the data, the subject order was sorted according to the mean of net metabolic cost rate reduction in FMCH and CCH mode. All data were processed with Matlab (R2018b, MathWorks) scripts.

E. Statistics

For each condition (i.e. transparent, FMCH and CCH), means and standard deviations of peak joint angle, muscle r.m.s EMG, net metabolic cost rate, exoskeleton torque, power and mechanical energy were computed across participants with standard deviation indicating inter-participant variability. Jarque-Bera test was used for checking if peak joint angle, muscle r.m.s EMG and net metabolic cost rate were normally distributed in each condition. If the data were normally distributed, one-way repeated measures analysis of variance (ANOVA) was performed across three conditions

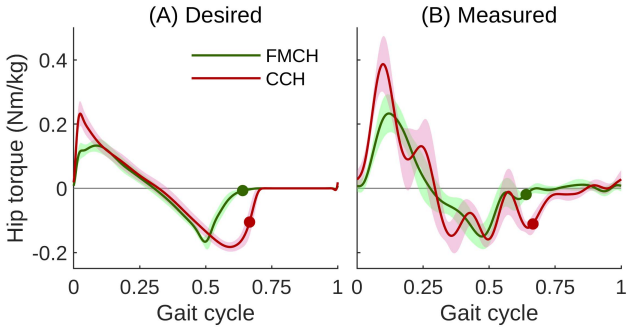

Fig. 4. The normalized hip extension/flexion torque (difference between the FMCH/CCH and the transparent mode) applied by exoskeleton. Positive values denote the extension torques. The desired and measured torques are shown in the subfigure (a) and (b), respectively. FMCH and CCH are shown in red and green color, respectively. Solid lines denote the mean value of all eight subjects. Error bands denote ±1 standard deviation. Circle markers indicate the toe-off.

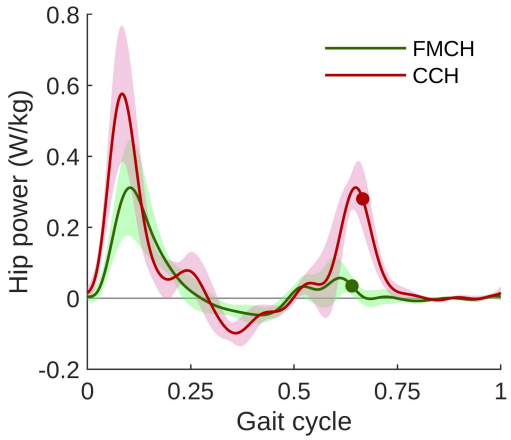

Fig. 5. The measured hip mechanical power (normalized to subject body mass) applied by the exoskeleton. FMCH and CCH are shown in green and red color, respectively. Solid lines denote the mean values of all eight subjects. Error bands denote ±1 standard deviation. Circle markers indicate the toe-off.

(i.e. transparent, FMCH and CCH). Otherwise the nonparametric Friedman test were performed. Mauchly test was used to evaluate sphericity. The Greenhouse-Geiser correction was applied if the sphericity assumption was violated. If the repeated measures ANOVA or the Friedman test indicated a significant effect, the paired t-test was used for *post hoc* tests. The paired t-test was performed between FMCH and CCH condition for exoskeleton peak torque, power and mechanical energy. p values less than or equal to 0.05 were considered as indicators of statistical significance. All statistical tests were conducted in Matlab (R2018b, MathWorks).

III. Results

A. Exoskeleton Torque and Power

CCH generated larger desired hip torque than FMCH for both extension and flexion (Fig. 4). The desired torque in CCH has much sharper increasing and decreasing edges compared to FMCH. The measured peak torque in FMCH is smaller than in CCH (0.149 ± 0.064 N m/kg, $p < 0.001$). Both FMCH and CCH generate similar hip torque pattern during mid-stance phase ($15 \sim 35\%$ of gait cycle), while the measured torque in CCH has larger oscillations in both stance phase and swing phase compared to FMCH. The peak hip extension torque in CCH occurs earlier than in FMCH, while the peak hip flexion torque in FMCH occurs earlier than in CCH.

Similar to the measured torque, the measured mechanical power in CCH also has more oscillations than FMCH. Compared to CCH, FMCH requires less mechanical peak power (0.603 ± 0.180 W m/kg in CCH, 0.322 ± 0.137 W m/kg in FMCH, $p < 0.001$) for the exoskeleton (Fig. 5). The averaged mechanical energy applied by the exoskeleton over one gait cycle in FMCH (0.1206 ± 0.0246 J m/kg) is also significantly ($p < 0.001$) lower than CCH (0.2069 ± 0.0287 J m/kg).

B. Joint Kinematics

The hip and knee join angle patterns during the gait cycle are similar in transparent, FMCH, and CCH mode. Compared to the transparent mode, the peak of the hip adduction angle is not significantly different in neither FMCH nor CCH mode. Hip maximum extension angle during stance phase in FMCH is significantly smaller than in transparent mode ($1.7° \pm 1.4°$, $p = 0.014$). Hip maximum flexion angle during swing phase in both FMCH and CCH is significantly different from the transparent mode (FMCH is $1.4° \pm 1.07°$ smaller, $p = 0.008$; CCH is $2.3° \pm 2.1°$ larger, $p = 0.019$). Knee maximum flexion angle during the flight phase in CCH is significantly larger than in the transparent mode ($6.2° \pm 3.0°$, $p < 0.001$). Both hip and knee joints in FMCH and CCH during the early stance phase ($0 \sim 20\%$ of gait cycle) extend faster than in transparent mode.

C. Muscle Activation

Fig. 7 shows the mean normalized EMG pattern across all eight subjects. All eight muscle activation patterns are similar between transparent, FMCH and CCH modes. There are no significant changes for the peak activation of all muslces.

The mean of normalized r.m.s EMG of all muscles which are attached to the thigh (i.e. GAS, VAS, REC, HAM and GLU) show reductions in FMCH (Fig. 8). HAM shows the largest reduction ($20.9 \pm 8.7\%$, $p < 0.001$) while REC activation keeps almost the same as the transparent in FMCH. GAS also shows significant reduction ($5.5 \pm 5.6\%$, $p = 0.028$) in FMCH compared to the transparent mode which is also shown in Fig. 7. GAS, VAS and GLU show similar amount of reductions in both FMCH and CCH.

Different subjects have different responses in terms of muscle activation to FMCH and CCH (Fig. 9). However, compared to CCH, FMCH has more consistent muscle responses. Compared to transparent mode, HAM activation has significant reduction for all subjects in FMCH. In contrast, only four subjects have HAM reduction in CCH (Fig. 9). Overall EMG reduction of all muscles is smaller in CCH than in FMCH. TIA is the least responsive muscle to both FMCH (three subjects) and CCH (four subjects) controllers. The changes in muscle

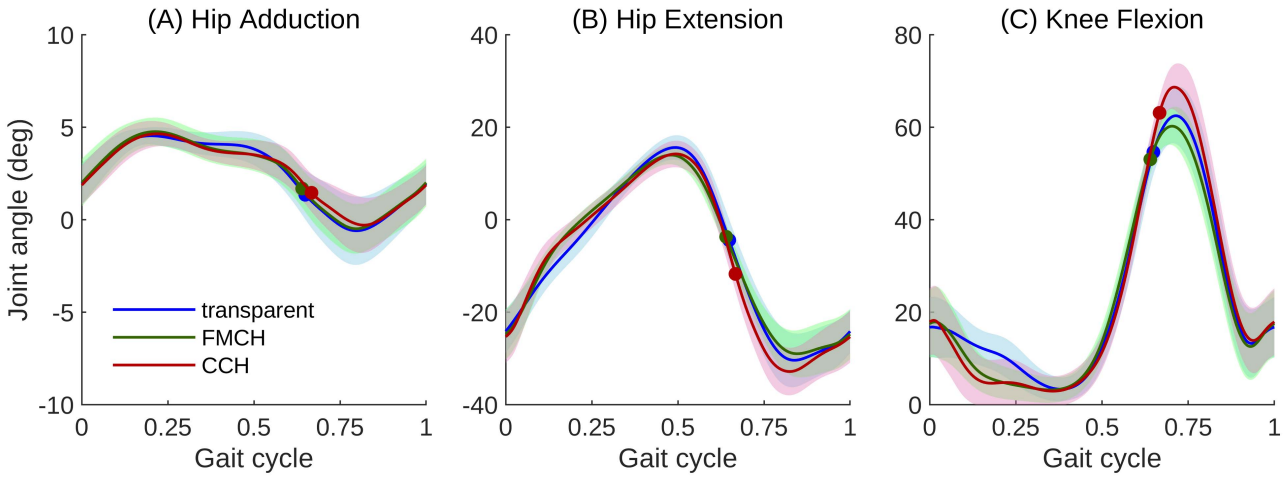

Fig. 6. Joint kinematics during the gait cycle. Hip adduction and extension are shown as positive in the subfigure (A) and (B). Knee flexion is shown as positive in the subfigure (C). Transparent, FMCH, and CCH mode walking are shown in blue, red, and green color, respectively. Solid lines denote the subject mean. Error bands denote ±1 standard deviation. Circle markers indicate the toe-off.

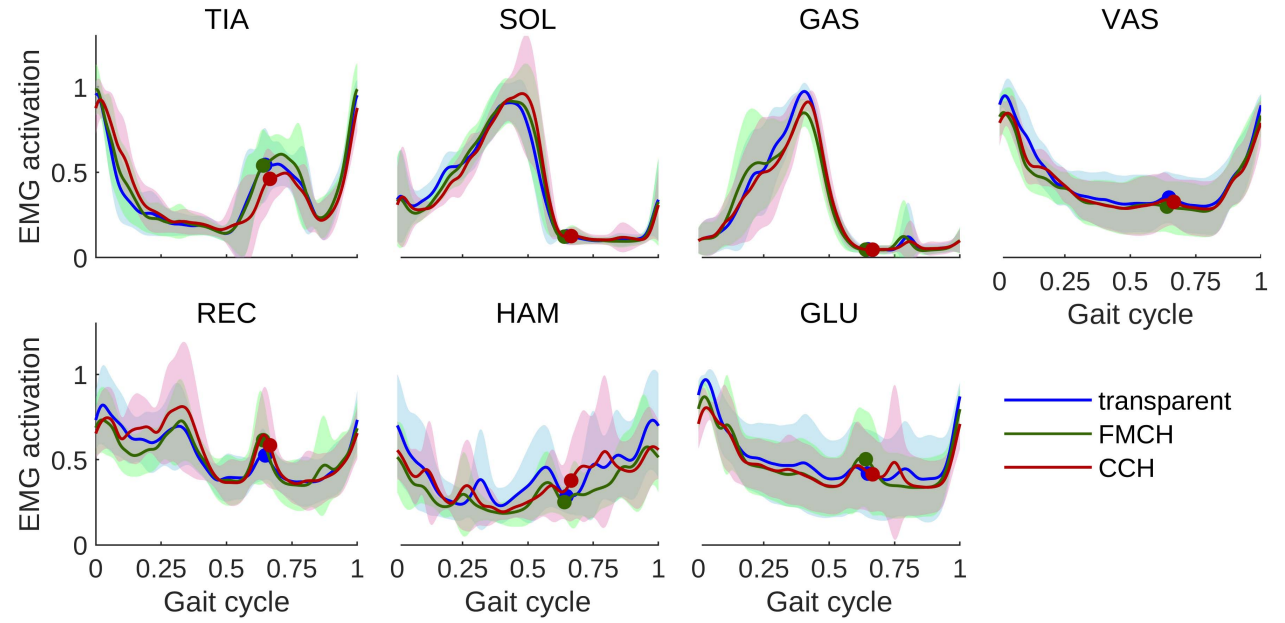

Fig. 7. Normalized electromyography (EMG) of tibialis anterior (TIA), soleus (SOL), gastrocnemius medialis (GAS), vastus medialis (VAS), rectus femoris (REC), hamstring (HAM), and gluteus maximus (GLU) muscle during the gait cycle. Solid lines denote the mean values of all eight subjects. Error bands denote ±1 standard deviation. Transparent, FMCH, and CCH mode walking are shown in blue, red, and green color, respectively. Circle markers indicate the toe-off.

activation varies quite a lot individually (e.g. SOL, REC and HAM) in CCH.

Subject 1 and 4 with high metabolic cost reduction show EMG reductions in all muscles except TIA which is not significant in FMCH. Subject 2 shows second highest metabolic cost reduction with FMCH has high reduction in VAS and HAM, but REC and GLU activation increased. Subject 1 and 3 with high metabolic cost reduction in CCH have an increase in muscles activation in three and two muscles, respectively.

D. Metabolic Cost

Compared to the transparent mode, seven out of eight subjects show a reduced net metabolic cost rate (Fig. 10) in both FMCH and CCH mode. The average reduction of all eight subjects in FMCH mode is $6.0 \pm 11.4\%$ which is not significant ($p = 0.128$), while the CCH mode has significant reduction of $7.8 \pm 6.8\%$ ($p = 0.018$). Subject 1 has the highest metabolic reduction in both FMCH (24.1%) and CCH (17.7%). Only subject 8 shows a metabolic increase in both FMCH (15.3%) and CCH (3.7%).

IV. Discussions

In this paper, a new bio-inspired reflex-based approach was presented and applied for control of an exoskeleton to assist human walking. With both modulated and fixed hip compliance controller, we found reductions in the average

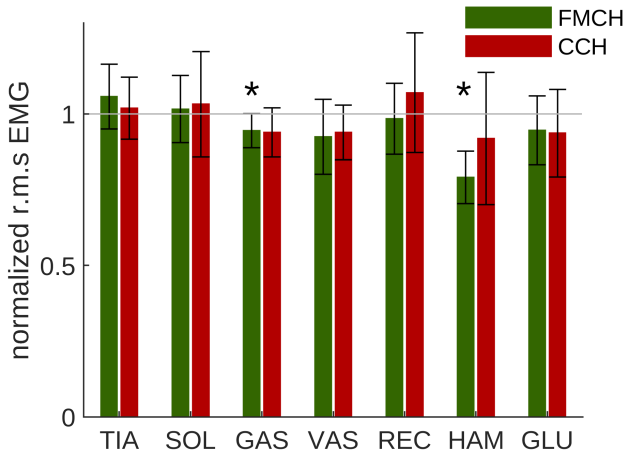

Fig. 8. Normalized root mean square electromyography (r.m.s. EMG) of tibialis anterior (TIA), soleus (SOL), gastrocnemius medialis (GAS), vastusmedialis (VAS), rectus femoris (REC), hamstring (HAM), and gluteus maximus (GLU) during the gait cycle. It is normalized to the r.m.s EMG in the transparent mode. The bar height denotes the mean values of all eight subjects. The error-bar denotes ±1 standard deviation. FMCH and CCH mode are shown in red and green bar, respectively. Asterisks indicate that the EMG reduction is significant compared to the transparent mode.

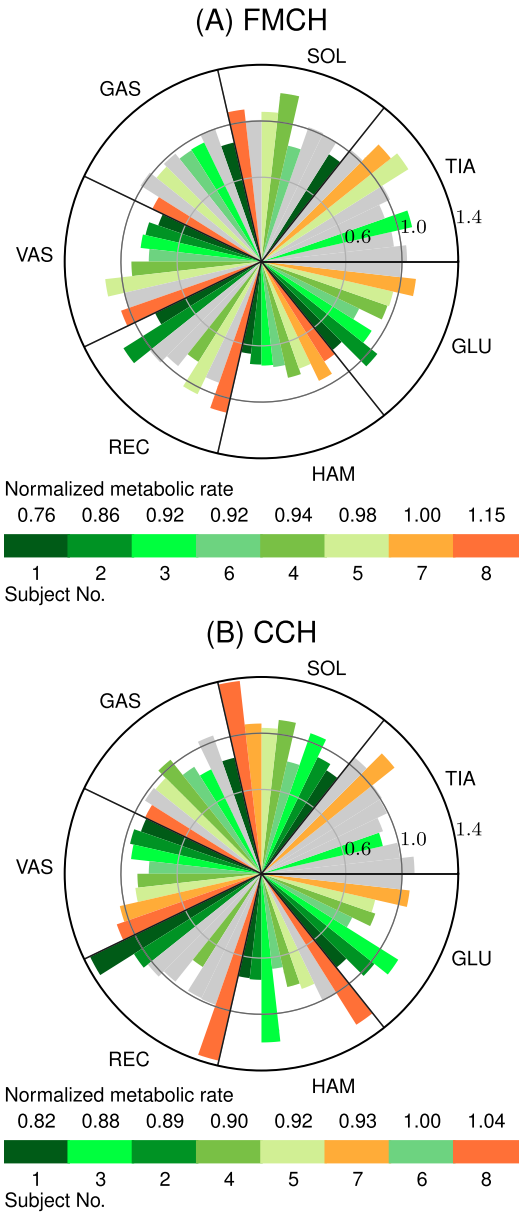

Fig. 9. Individual normalized root mean square electromyography (r.m.s EMG) of tibialis anterior (TIA), soleus (SOL), gastrocnemius medialis (GAS), vastus medialis (VAS), rectus femoris (REC), hamstring (HAM), and gluteus maximus (GLU) muscle of all eight subjects walking with (A) FMCH controller, and (B) CCH controller. The r.m.s EMG is represented as the radius. The color denotes the subject specific normalized metabolic rate. The r.m.s EMG is normalized to the transparent mode (e.g. the muscle activation is reduced in FMCH mode compared to transparent mode if the bar height is smaller than 1). Different subjects are denoted with different colors. Gray color denotes that the muscle activation is not significantly different to the transparent mode. Normalized net metabolic cost rate value of each subject is shown above the legend bar. Subject No. is shown below the legend bar.

net metabolic rate and muscle activation. Compared to the fixed hip compliance, modulation using leg force results in more natural kinematic behavior, more consistent reduction in muscle activities, smoother motor torques and less peak power from the exoskeleton.

It has been shown that the muscle positive force feedback is beneficial for the motion stability in locomotor control [52]. The modulated hip compliance based on leg force controller mimics this force feedback pathway during human gait [10]. We have previously investigated FMCH bio-inspired posture control concept using biarticular thigh actuation for assistance with an exosuit using a neuromuscular model [46]. Additionally, we implemented this concept in an exoskeleton by emulating biarticular muscles with single joint actuation at hip and knee [45], in contrast to here presented study which is focused on hip actuation. Although the trunk angle is fixed in this study, the posture control based assistance can still result in reduction in both muscle activation and metabolic costs. This could be because human hip control remains consistent even if the posture control is not an issue.

A. Joint Kinematic Patterns Are Preserved

From analyzing the kinematic behavior with the exoskeleton, the joint angle patterns do not change too much (e.g. less than 10% difference in joint angle peaks) in all three control schemes (i.e. transparent, FMCH, and CCH). This demonstrates that both FMCH and CCH can preserve the kinematic patterns. The hip joint maximum extension and flexion angle in FMCH is a bit smaller than in the transparent mode. In contrast, CCH results in larger maximum flexion angle for both hip and knee joint compared to the transparent mode. This suggests that FMCH only affects the hip flexion/extension joint kinematics while CCH affects both hip and knee joint kinematics.

Another finding is prolonged straight knee configurations during stance phase with both FMCH and CCH (Fig. 6). This indicates that providing parallel hip compliance at the beginning of stance phase is beneficial for human gait as it supports straight stance leg configuration which can reduce

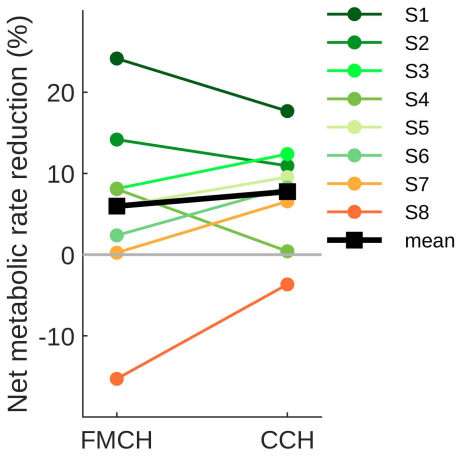

Fig. 10. Net metabolic cost rate reduction of all eight subjects in the FMCH and CCH mode compared to the transparent mode. S1 to S8 indicate eight subjects. Mean reduction are shown in black color.

knee extensors activation and result in lower metabolic costs. In a study using a clutchable ankle spring, 7.2% metabolic cost reduction during walking [53] was found. This is in agreement with our results that switchable joint compliance (both FMCH and CCH, Fig. 10) can provide metabolic benefits during human gait. But it is important to note that this could also lead to load the knee joint in the straight configuration. A knee assistance control could be added in the future to prevent this.

B. FMCH Based Controller Is More Efficient

The efficiency of a control approach can be evaluated based on the energy consumption not only of the human body but also of the assistive device. Although both FMCH and CCH provide almost the same amount of metabolic cost rate reduction (Fig. 10), the mechanical peak power applied by the exoskeleton over one gait cycle in CCH is about twice as high as in FMCH (Fig. 5). This suggests that control of the exoskeleton with the FMCH approach is more efficient than the CCH. The oscillations in the hip power patterns in CCH is originated from the hip torque oscillations. In fact, both FMCH and CCH generate human-like hip torque pattern, but the measured torque in FMCH is much smoother than CCH (Fig. 4). Such fluctuations are due to sharp changes in the desired hip torque with CCH control right after TD (Fig. 4). This indicates that the bio-inspired FMCH approach provides benefits to reduce the peak torque and power at the hip joint and a smoother profile of the hip torque pattern. This facilitates not only human gait but also the implementation in assistive devices such as exoskeletons.

Energy injection in the first half of the stance phase can contribute to the postural control [43]. The hip extension torques lead to a vertical alignment of the GRF vector and thus reduces the risk of foot slipping at early ground contact. Thus, energy injection at the hip joint right after TD can improve traction control in legged locomotion while decelerating the upper body forward rotation. This initiates the pendulum-like body movement described in the VPP concept [43]. Furthermore, this active hip extension torque in early stance phase can support not only the upright trunk posture but also the forward acceleration of the contralateral leg to initiate the swing movement. In the second half of stance phase, first the exo generates negative power (significantly smaller compared to the positive power in the first half). This contributes to keep the upper body upright by dissipating part of the injected energy. Afterwards, the hip supports leg swing with active hip flexion torque and accelerating the thigh forward. This results in a second energy injection phase (Fig. 5), which has similar effects as the positive power in the first half of stance phase and also supports the pre-swing movement. Hence, the proposed control methods contribute to the forward rotation of the swing leg, which is driven by the hip torques during stance phase.

C. FMCH Based Controller Has Higher Consistency in EMG Responses

Analyzing muscle activation (Fig. 8 and Fig. 9) demonstrates successful transfer and application of bio-inspired control models based on human walking dynamics. The following general behaviours are observable from muscle reactions to assistance: 1) consistent and significant reduction in HAM and GAS muscle for all subjects using FMCH method (Fig. 8 and 9); 2) non-significant but consistent reductions in mean normalized activity in all other hip and knee muscles in both FMCH and CCH except REC in CCH (Fig. 8); 3) more consistent muscle responses (Fig. 9) and higher reduction in muscle activities (Fig. 8) in different subjects with FMCH compared to CCH. These results show that the leg force feedback improves assistance level with respect to reduction in muscle activation, as predicted by our bio-inspired gait models [46]. In line with improving locomotion function (e.g. regarding kinematics and power consumption), by analyzing activities in different muscles, the exoskeleton can provide essential assistance to a specific muscle group (e.g. HAM). Significant reductions in HAM and GAS muscles using FMCH method are in agreement with previous findings in [45] using two-joint actuation at hip and knee. In our compliant hip approaches, the applied torque to the upper part of thigh segment has positive effects on the muscles acting on this segment. Comparison between CCH and FMCH in Fig. 8 shows clear reductions in thigh biarticular muscles activities, obtained by using leg force feedback in FMCH. This is in agreement with the implementation of VPP concept through FMCH and biarticular thigh actuation in simulated walking models [11] and a bipedal robot [54].

Higher consistency between different subjects' muscle responses in FMCH compared to CCH (Fig. 9) shows that the feedback (reflex) control enhances the adaptability of the user to the assistive device. Assistance of the exoskeleton after TD and at the push-off phase supports the pre-swing leg function as well. In addition, support of the exoskeleton in the second half of stance phase contributes to redirecting the CoM velocity before TD of the contralateral swing leg. This is in line with the significant reduction in hip extensor muscles (HAM and GLU) during swing phase.

As gait assistance needs appropriate interaction with human movement, bio-inspired design and control approaches provide clear advantages. In the recent years, introducing wearable (soft) assistive devices called exosuits [55]–[57] was a breakthrough enabling novel bio-inspired designs for assistive systems. In this paper, we introduced a simple bio-inspired control method which enables a new approach for assistance toward a more collaborative instead of master-slave relation between human and machine. The novel FMCH based controller reacts to human action within a bio-inspired control framework. Previous experimental and simulation studies have shown that FMCH is a feasible control concept for balance [10], [11]. Here, we found that the exoskeleton can assist human by using the same feedback design. Our template based approach avoids the model complexity which is a common drawback of such approaches [12]. It is the first implementation of such a novel method on a single (hip) joint actuated exoskeleton demonstrated beneficial outcomes regarding reducing metabolic costs and muscle activities compared to similar studies (only with hip joint assistance) on exoskeletons [35], [36], [58] or exosuits [56], [59].

D. Limitations

In this study, we are focusing on assisting the hip joints to investigate the benefits of FMCH based controller for walking energetics. Although the FMCH controller is a bio-inspired posture control concept, the posture stability and balance performance during walking cannot be investigated because of the hardware limitations of LOPES II (the trunk angle is fixed and set to zero during walking). This feature can be investigated with other hip exoskeletons in the future.

Another limitation of this study is that we used a fixed control parameter set for all subjects. Although the parameters were normalized to subject body weight and body height, it could still lower the performance of the proposed method. This is because different subjects have different gait characteristics which are not related to individual body weight and height (e.g. hip rest angle). This could explain the different responses to the controller across different subjects. For instance, subject 8 showed increased net metabolic cost rate in both FMCH and CCH while all other subjects showed the opposite (Fig. 10). Studies have shown that applying subject specific control parameters with human-in-the-loop optimization approach can improve the level of assistance [57], [60]. In further research our FMCH controller could be combined with human-in-the-loop optimization method to find the individualized control parameters.

Using a minor control interference, as employing leg force to proportionally tune hip stiffness (in FMCH), provides clear advantages compared to the constant hip stiffness design (CCH). A simple proportional gain modulation is sufficient to achieve the observed enhancement in assistance. With our findings we have shown that the FMCH control concept, which is originally for balance control, can provide assistance for walking gait. Still, the swing leg control is one missing part in the proposed method as the exoskeleton operates in transparent mode during swing phase. We have started to extend our bio-inspired methodology to assist subjects during swing phase (e.g. using the biarticular mechanism as presented in [61]). In that respect, a preliminary version of an exosuit with biarticular thigh muscles was developed [46]. Mimicking muscle properties such as compliance, morphology, biarticular actuation and reflex-based (e.g. force feedback in FMCH) control are important design and control features of novel bio-inspired assistive devices.

REFERENCES

[1] M. Grimmer, R. Riener, C. J. Walsh, and A. Seyfarth, "Mobility related physical and functional losses due to aging and disease—A motivation for lower limb exoskeletons," *J. Neuroeng. Rehabil.*, vol. 16, no. 1, p. 2, Dec. 2019.

[2] I. E. Brown and G. E. Loeb, *A Reductionist Approach to Creating and Using Neuromusculoskeletal Models*. New York, NY, USA: Springer, 2000, pp. 148–163.

[3] A. J. Ijspeert, "Central pattern generators for locomotion control in animals and robots: A review," *Neural Netw.*, vol. 21, no. 4, pp. 642–653, 2008.

[4] V. Dietz, "Proprioception and locomotor disorders," *Nature Rev. Neurosci.*, vol. 3, pp. 781–790, Oct. 2002.

[5] S. Harkema *et al.*, "Effect of epidural stimulation of the lumbosacral spinal cord on voluntary movement, standing, and assisted stepping after motor complete paraplegia: A case study," *Lancet*, vol. 377, pp. 1938–1947, Jun. 2011.

[6] Y. Gerasimenko, R. R. Roy, and V. R. Edgerton, "Epidural stimulation: Comparison of the spinal circuits that generate and control locomotion in rats, cats and humans," *Exp. Neurol.*, vol. 209, no. 2, pp. 417–425, Feb. 2008.

[7] E. Bizzi, V. C. K. Cheung, A. D'Avella, P. Saltiel, and M. Tresch, "Combining modules for movement," *Brain Res. Rev.*, vol. 57, no. 1, pp. 125–133, Jan. 2008.

[8] H. Geyer and H. Herr, "A muscle-reflex model that encodes principles of legged mechanics produces human walking dynamics and muscle activities," *IEEE Trans. Neural Syst. Rehabil. Eng.*, vol. 18, no. 3, pp. 263–273, Jun. 2010.

[9] S. Song and H. Geyer, "A neural circuitry that emphasizes spinal feedback generates diverse behaviours of human locomotion," *J. Physiol.*, vol. 593, no. 16, pp. 3493–3511, Aug. 2015.

[10] M. A. Sharbafi and A. Seyfarth, "FMCH: A new model for human-like postural control in walking," in *Proc. IEEE/RSJ Int. Conf. Intell. Robots Syst. (IROS)*, Sep./Oct. 2015, pp. 5742–5747.

[11] M. A. Sharbafi, A. Seyfarth, and G. Zhao, "Locomotor sub-functions for control of assistive wearable robots," *Frontiers Neurorobot.*, vol. 11, p. 44, Sep. 2017.

[12] T. Yan, M. Cempini, C. M. Oddo, and N. Vitiello, "Review of assistive strategies in powered lower-limb orthoses and exoskeletons," *Robot. Auto. Syst.*, vol. 64, pp. 120–136, Feb. 2015.

[13] D. Sanz-Merodio, M. Cestari, J. C. Arevalo, and E. Garcia, "Control motion approach of a lower limb orthosis to reduce energy consumption," *Int. J. Adv. Robot. Syst.*, vol. 9, no. 6, p. 232, 2012.

[14] Y. Sankai, "HAL: Hybrid assistive limb based on cybernics," in *Robotics Research*. Berlin, Germany: Springer, 2010, pp. 25–34.

[15] P. D. Neuhaus, J. H. Noorden, T. J. Craig, T. Torres, J. Kirschbaum, and J. E. Pratt, "Design and evaluation of mina: A robotic orthosis for paraplegics," in *Proc. IEEE Int. Conf. Rehabil. Robot. (ICORR)*, Jun./Jul. 2011, pp. 1–8.

[16] S. Wang *et al.*, "Design and control of the MINDWALKER exoskeleton," *IEEE Trans. Neural Syst. Rehabil. Eng.*, vol. 23, no. 2, pp. 277–286, Mar. 2015.

[17] A. Esquenazi, M. Talaty, A. Packel, and M. Saulino, "The ReWalk powered exoskeleton to restore ambulatory function to individuals with thoracic-level motor-complete spinal cord injury," *Amer. J. Phys. Med. Rehabil.*, vol. 91, no. 11, pp. 911–921, 2012.

[18] K. A. Strausser and H. Kazerooni, "The development and testing of a human machine interface for a mobile medical exoskeleton," in *Proc. IEEE/RSJ Int. Conf. Intell. Robots Syst. (IROS)*, Sep. 2011, pp. 4911–4916.

[19] A. T. Asbeck, R. J. Dyer, A. F. Larusson, and C. J. Walsh, "Biologically-inspired soft exosuit," in *Proc. IEEE Int. Conf. Rehabil. Robot. (ICORR)*, Jun. 2013, pp. 1–8.

[20] C. J. Walsh, K. Pasch, and H. Herr, "An autonomous, underactuated exoskeleton for load-carrying augmentation," in *Proc. IEEE/RSJ Int. Conf. Intell. Robots Syst.*, Oct. 2006, pp. 1410–1415.

[21] Y. Mori, J. Okada, and K. Takayama, "Development of a standing style transfer system 'ABLE' for disabled lower limbs," *IEEE/ASME Trans. Mechatronics*, vol. 11, no. 4, pp. 372–380, Aug. 2006.

[22] F. Chen, Y. Yu, Y. Ge, and Y. Fang, "WPAL for human power assist during walking using dynamic equation," in *Proc. Int. Conf. Mechatronics Autom. (ICMA)*, Aug. 2009, pp. 1039–1043.

[23] S.-H. Hyon, J. Morimoto, T. Matsubara, T. Noda, and M. Kawato, "XoR: Hybrid drive exoskeleton robot that can balance," in *Proc. IEEE/RSJ Int. Conf. Intell. Robots Syst. (IROS)*, Sep. 2011, pp. 3975–3981.

[24] H. Kawamoto *et al.*, "Voluntary motion support control of robot suit HAL triggered by bioelectrical signal for hemiplegia," in *Proc. Annu. Int. Conf. IEEE Eng. Med. Biol. (EMBC)*, Aug./Sep. 2010, pp. 462–466.

[25] R. Ronsse *et al.*, "Oscillator-based assistance of cyclical movements: Model-based and model-free approaches," *Med. Biol. Eng. Comput.*, vol. 49, no. 10, p. 1173, Oct. 2011.

[26] F. Giovacchini, F. Vannetti, M. Fantozzi, M. Cempini, M. Cortese, A. Parri, T. Yan, D. Lefeber, and N. Vitiello, "A light-weight active orthosis for hip movement assistance," *Robot. Auton. Syst.*, vol. 73, pp. 123–134, Nov. 2015.

[27] N. L. Tagliamonte, F. Sergi, G. Carpino, D. Accoto, and E. Guglielmelli, "Human-robot interaction tests on a novel robot for gait assistance," in *Proc. IEEE Int. Conf. Rehabil. Robot. (ICORR)*, Jun. 2013, pp. 1–6.

[28] T. Matsubara, A. Uchikata, and J. Morimoto, "Full-body exoskeleton robot control for walking assistance by style-phase adaptive pattern generation," in *Proc. IEEE/RSJ Int. Conf. Intell. Robots Syst. (IROS)*, Oct. 2012, pp. 3914–3920.

[29] X. Zhang and M. Hashimoto, "Synchronization based control for walking assist suit-evaluation on synchronization and assist effect," *Key Eng. Mater.*, vol. 464, pp. 115–118, Jan. 2011.

[30] R. Ronsse *et al.*, "Oscillator-based assistance of cyclical movements: Model-based and model-free approaches," *Med. Biol. Eng. Comput.*, vol. 49, no. 10, pp. 1173–1185, 2011.

[31] C. Fleischer and G. Hommel, "A human–exoskeleton interface utilizing electromyography," *IEEE Trans. Robot.*, vol. 24, no. 4, pp. 872–882, Aug. 2008.

[32] J. A. Norris, K. P. Granata, M. R. Mitros, E. M. Byrne, and A. P. Marsh, "Effect of augmented plantarflexion power on preferred walking speed and economy in young and older adults," *Gait Posture*, vol. 25, no. 4, pp. 620–627, Apr. 2007.

[33] P. C. Kao, C. L. Lewis, and D. P. Ferris, "Invariant ankle moment patterns when walking with and without a robotic ankle exoskeleton," *J. Biomech.*, vol. 43, no. 2, pp. 203–209, Jan. 2010.

[34] H. Kazerooni, R. Steger, and L. Huang, "Hybrid control of the Berkeley lower extremity exoskeleton (BLEEX)," *Int. J. Robot. Res.*, vol. 25, nos. 5–6, pp. 561–573, May/Jun. 2006.

[35] Q. Wu, X. Wang, F. Du, and X. Zhang, "Design and control of a powered hip exoskeleton for walking assistance," *Int. J. Adv. Robotic Syst.*, vol. 12, no. 3, p. 18, Mar. 2015.

[36] T. Lenzi, M. C. Carrozza, and S. K. Agrawal, "Powered hip exoskeletons can reduce the user's hip and ankle muscle activations during walking," *IEEE Trans. Neural Syst. Rehabil. Eng.*, vol. 21, no. 6, pp. 938–948, Nov. 2013.

[37] H. He and K. Kiguchi, "A study on EMG-based control of exoskeleton robots for human lower-limb motion assist," in *Proc. 6th Int. Special Topic Conf. Inf. Technol. Appl. Biomed.*, Nov. 2007, pp. 292–295.

[38] K. Kong and D. Jeon, "Design and control of an exoskeleton for the elderly and patients," *IEEE/ASME Trans. Mechatronics*, vol. 11, no. 4, pp. 428–432, Aug. 2006.

[39] T.-J. Yeh, M.-J. Wu, T.-J. Lu, F.-K. Wu, and C.-R. Huang, "Control of McKibben pneumatic muscles for a power-assist, lower-limb orthosis," *Mechatronics*, vol. 20, no. 6, pp. 686–697, Sep. 2010.

[40] A. R. Wu *et al.*, "An adaptive neuromuscular controller for assistive lower-limb exoskeletons: A preliminary study on subjects with spinal cord injury," *Frontiers Neurorobot.*, vol. 11, p. 30, Jun. 2017.

[41] F. Dzeladini *et al.*, "Effects of a neuromuscular controller on a powered ankle exoskeleton during human walking," in *Proc. 6th IEEE Int. Conf. Biomed. Robot. Biomechatronics (BioRob)*, Jun. 2016, pp. 617–622.

[42] V. R. Garate *et al.*, "Walking assistance using artificial primitives: A novel bioinspired framework using motor primitives for locomotion assistance through a wearable cooperative exoskeleton," *IEEE Robot. Autom. Mag.*, vol. 23, no. 1, pp. 83–95, Mar. 2016.

[43] H.-M. Maus, S. W. Lipfert, M. Gross, J. Rummel, and A. Seyfarth, "Upright human gait did not provide a major mechanical challenge for our ancestors," *Nature Commun.*, vol. 1, p. 70, Sep. 2010.

[44] M. A. Sharbafi and A. Seyfarth, "Stable running by leg force-modulated hip stiffness," in *Proc. IEEE Int. Conf. Biomed. Robot. Biomechatronics*, Aug. 2014, pp. 204–210.

[45] G. Zhao, M. Sharbafi, M. Vlutters, E. Van Asseldonk, and A. Seyfarth, "Template model inspired leg force feedback based control can assist human walking," in *Proc. Int. Conf. Rehabil. Robot. (ICORR)*, Jul. 2017, pp. 473–478.

[46] M. A. Sharbafi, H. Barazesh, M. Iranikhah, and A. Seyfarth, "Leg force control through biarticular muscles for human walking assistance," *Frontiers NeuroRobot.*, vol. 12, p. 39, Jul. 2018.

[47] D. J. Farris and G. S. Sawicki, "The mechanics and energetics of human walking and running: A joint level perspective," *J. Roy. Soc. Interface*, vol. 9, no. 66, pp. 110–118, Jan. 2012.

[48] J. Meuleman, E. van Asseldonk, G. van Oort, H. Rietman, and H. van der Kooij, "LOPES II—Design and evaluation of an admittance controlled gait training robot with shadow-leg approach," *IEEE Trans. Neural Syst. Rehabil. Eng.*, vol. 24, no. 3, pp. 352–363, Mar. 2016.

[49] M. Vlutters, E. H. F. van Asseldonk, and H. van der Kooij, "Center of mass velocity-based predictions in balance recovery following pelvis perturbations during human walking," *J. Experim. Biol.*, vol. 219, no. 10, pp. 1514–1523, May 2016.

[50] J. A. Zeni, J. G. Richards, and J. S. Higginson, "Two simple methods for determining gait events during treadmill and overground walking using kinematic data," *Gait Posture*, vol. 27, no. 4, pp. 710–714, 2008.

[51] J. M. Brockway, "Derivation of formulae used to calculate energy expenditure in man," *Human Nutrition. Clin. Nutrition*, vol. 41, no. 6, pp. 463–471, 1987.

[52] A. Prochazka, D. Gillard, and D. J. Bennett, "Positive force feedback control of muscles," *J. Neurophysiol.*, vol. 77, no. 6, pp. 3226–3236, Jun. 1997.

[53] S. H. Collins, M. B. Wiggin, and G. S. Sawicki, "Reducing the energy cost of human walking using an unpowered exoskeleton," *Nature*, vol. 522, no. 7555, p. 212, 2015.

[54] M. A. Sharbafi *et al.*, "A new biarticular actuator design facilitates control of leg function in BioBiped3," *Bioinspiration Biomimetics*, vol. 11, no. 4, Jul. 2016, Art. no. 046003.

[55] A. T. Asbeck, K. Schmidt, and C. J. Walsh, "Soft exosuit for hip assistance," *Robot. Auton. Syst.*, vol. 73, pp. 102–110, Nov. 2015.

[56] A. T. Asbeck, S. M. M. D. Rossi, K. G. Holt, and C. J. Walsh, "A biologically inspired soft exosuit for walking assistance," *Int. J. Robot. Res.*, vol. 34, no. 6, pp. 744–762, Mar. 2015.

[57] Y. Ding, M. Kim, S. Kuindersma, and C. J. Walsh, "Human-in-the-loop optimization of hip assistance with a soft exosuit during walking," *Sci. Robot.*, vol. 3, no. 15, Feb. 2018, Art. no. eaar5438.

[58] K. Seo, J. Lee, Y. Lee, T. Ha, and Y. Shim, "Fully autonomous hip exoskeleton saves metabolic cost of walking," in *Proc. IEEE Int. Conf. Robot. Autom. (ICRA)*, May 2016, pp. 4628–4635.

[59] A. J. Young, H. Gannon, and D. P. Ferris, "A biomechanical comparison of proportional electromyography control to biological torque control using a powered hip exoskeleton," *Frontiers Bioeng. Biotechnol.*, vol. 5, p. 37, Jun. 2017.

[60] J. Zhang *et al.*, "Human-in-the-loop optimization of exoskeleton assistance during walking," *Science*, vol. 356, no. 6344, pp. 1280–1284, Jun. 2017.

[61] M. A. Sharbafi, A. M. N. Rashty, C. Rode, and A. Seyfarth, "Reconstruction of human swing leg motion with passive biarticular muscle models," *Human Movement Sci.*, vol. 52, pp. 96–107, Apr. 2017.